Influence of cell wall curvature radius and adhesive layer on the effective elastic out-of-plane properties of hexagonal honeycombs

Stefan SOROHAN*,[1], Dan Mihai CONSTANTINESCU[1], Marin SANDU[1], Adriana Georgeta SANDU[1]

*Corresponding author
[1]University "POLITEHNICA" of Bucharest, Department of Strength of Materials, Splaiul Independenţei 313, 060042, Bucharest, Romania,
stefan.sorohan@upb.ro*, d_constantinescu@yahoo.com, marin_sandu@yahoo.com, adriana.sandu@upb.ro

DOI: 10.13111/2066-8201.2018.10.4.14

Received: 30 October 2018/ Accepted: 26 November 2018/ Published: December 2018

International Conference of Aerospace Sciences "AEROSPATIAL 2018"
25 - 26 October 2018, Bucharest, Romania, (held at INCAS, B-dul Iuliu Maniu 220, sector 6)
Section 4 – Materials and Structures

Abstract: *Numerical modeling of honeycomb structures in aerospace engineering is too tedious and time consuming. The homogenization of these structures permits to obtain an equivalent orthotropic homogeneous solid and its elastic effective properties and thus realizing very efficient simulations. In a sandwich structure the most important effective constants of the core are the out-of-plane shear moduli G_{23} and G_{13}. These particular effective constants can be obtained analytically, numerically or, if available, can be taken from the producer's data sheets. In the last case they are generally obtained experimentally, but only for some particular thicknesses of the cores and sandwich faces. The analytical models usually neglect the curvature radius of the cell walls and the adhesive layer influence by using some additional hypotheses. In this paper a general parameterization of commercial honeycombs is first discussed. Then, neglecting the skin effect and considering the rigid skin effect, the out-of-plane properties of the core are obtained using a finite element analysis of a representative volume element. The numerical results are analyzed by comparing them to the ones given by the existing analytical models and/or experimental data and their advantages and pitfalls are discussed and explained. The results provide new insights into understanding the mechanics of honeycombs.*

Key Words: *hexagonal honeycombs, node bond adhesive, Finite Element Analysis, effective elastic properties, adhesive thickness and fillet.*

1. INTRODUCTION

Honeycomb structures had found widespread applications in various fields as aerospace engineering, automotive, mechanical engineering, chemical engineering etc. Hexagonal honeycombs with double walls attached along the ribbon direction are called sometimes *commercial honeycombs*. The most important feature of the core is its relative density defined as the ratio between the effective density of the honeycomb material and that of the material from which the cell walls are made. The relative density can vary from 0.001 to,

generally, 0.4 [1, 2]. A variety of materials have been used as basic materials to fabricate honeycombs, including paperboard, fiberglass, carbon fiber reinforced plastic, Nomex or Kevlar reinforced plastic, polypropylene and metals, mainly aluminum and steel.

By using the finite element method, the explicit modeling of the complete core leads to a significant increase of finite elements and degrees of freedom, therefore increasing the computational effort without real benefits for some practical problems. Usually, in a finite element analysis (FEA), the macroscopic model of a panel can be modelled as a layered composite Shell with sandwich option or as a solid structure in which the core is discretized with orthotropic brick elements [3]. The reliability of the continuum model strongly depends on the accuracy of the effective core properties. If the honeycomb core is used in sandwich panels then the effective material properties are to be determined by considering the effect of the skins which are usually considered as being rigid. However, for the experimental determination of the in-plane elastic properties the honeycomb is tested without skins as done by Balawi and Abot [4] and by Karakoç and Freund [5]. Consequently, two categories of effective elastic constants can be evidenced: by neglecting the skin effect and by considering the rigid skin effect [6, 7].

Many analytical relations for establishing the effective mechanical properties estimations are considered in the literature [2, 8]. Gibson and Ashby summarized the analytical formulas for relative density and the in-plane and out-of-plane properties of commercial honeycombs but by neglecting the curvature radius at the walls intersection and the adhesive layer presence at the cell nodes. Masters and Evans [8] were the first to consider the radius of curvature at the intersection of the cell walls in an indirect way, that is by considering the hinging mode deformation, difficult to be generalized for various types of commercial honeycombs. In many researches, including new papers, analytical and/or numerical models consider the honeycombs without radii of curvature, as done in [6, 7, 9–11]. As to include the effect of the radius of curvature in establishing the effective elastic constants of composite honeycombs, recent works [12–14], make use of the modeling and simulation with finite elements. However, FEA implies a considerable calculus effort both in design and in various situations in which sensitivity analyses are required. Developing analytical relations for obtaining the effective elastic constants of honeycombs for which the real geometry is of real interest is a complex task. For in-plane effective constants, Sorohan et al. [15] obtained some particular formulas using the beam theory. For out-of-plane effective constants which consider the detailed geometry of hexagonal honeycombs there are not yet some simple formulas and, in this paper, the finite element method is used.

This research is dedicated to numerically obtaining all five out-of-plane effective elastic properties of the hexagonal honeycomb core considering the rigid skin effect and neglecting the skin effect, and by considering the radius of curvature at cell wall intersection and the adhesive layer at nodes.

2. BASICS OF HOMOGENIZATION CONCEPT

The effective elastic mechanical properties of honeycombs can be obtained starting with the isotropic constants of the core (solid, with subscript abbreviation *s*) material E_s – Young's modulus and v_s –Poisson's ratio [2]. In this paper, the similar properties of the adhesive E_a and v_a are necessary. The explicit topology of the commercial core structure is presented in Fig. 1. For an equivalent *orthotropic material*, with the principal directions along the axes of the system *OXYZ*, according to the generalized Hooke's law, it yields $\bar{\boldsymbol{\varepsilon}} = \boldsymbol{S}\,\bar{\boldsymbol{\sigma}}$, where $\bar{\boldsymbol{\varepsilon}}$ and $\bar{\boldsymbol{\sigma}}$ are the volume averaged strain and the volume averaged stress vector of the material unit

cell, respectively and ***S*** is the compliance matrix which includes the effective elastic mechanical properties [2].

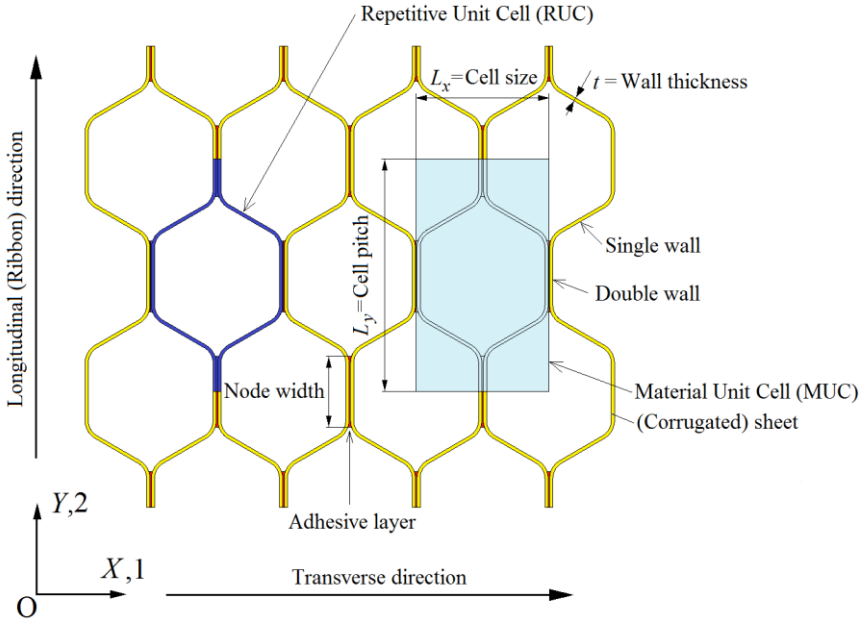

Fig. 1 – Part of the hexagonal honeycomb cell model: global system of coordinates, periodic cells, the repetitive unit cell, the homogeneous material unit cell and some of usual nomenclature

This relation in expanded form, using the Voigt's notation, when only out-of-plane stresses are non-zero, is

$$\begin{Bmatrix} \bar{\varepsilon}_z \\ \bar{\gamma}_{yz} \\ \bar{\gamma}_{xz} \end{Bmatrix} = \begin{bmatrix} \frac{1}{E_3} & 0 & 0 \\ 0 & \frac{1}{G_{23}} & 0 \\ 0 & 0 & \frac{1}{G_{13}} \end{bmatrix} \begin{Bmatrix} \bar{\sigma}_z \\ \bar{\tau}_{yz} \\ \bar{\tau}_{xz} \end{Bmatrix}. \tag{1}$$

If only one component of the stress vector is non-zero in (1), then the components of the compliance matrix may be obtained according to the definition of the elastic moduli and Poisson's ratios in Table 1.

Table 1 – Definition of out-of-plane elastic moduli and Poisson's ratios for an orthotropic material

Load case	Non-zero averaged stress	Elastic moduli	Poisson's ratios
1	$\bar{\sigma}_z$	$E_3 = \frac{\bar{\sigma}_z}{\bar{\varepsilon}_z}$	$\nu_{31} = -\frac{\bar{\varepsilon}_x}{\bar{\varepsilon}_z}$; $\nu_{32} = -\frac{\bar{\varepsilon}_y}{\bar{\varepsilon}_z}$
2	$\bar{\tau}_{yz}$	$G_{23} = \frac{\bar{\tau}_{yz}}{\bar{\gamma}_{yz}}$	-
3	$\bar{\tau}_{xz}$	$G_{13} = \frac{\bar{\tau}_{xz}}{\bar{\gamma}_{xz}}$	-

3. GENERAL REMARKS

Cell configuration of honeycombs depends on application requirements and may be available in different shapes [16, 17]. From existing various commercial cell configurations, only hexagonal honeycomb cells are discussed in this paper.

3.1 Commercial honeycombs

According to Kindinger [18], four primary manufacturing methods are used to produce a honeycomb: adhesive bonding and expansion; corrugation and adhesive bonding; corrugation and braze welding; extrusion. The most common manufacturing method is adhesive bonding and expansion. In the honeycomb industry the bonded portion of a honeycomb cell is called the node, while the single-sheet portion is called a free cell wall. In a cell, two of the six walls have roughly a double thickness (see Fig. 1).

When defining a honeycomb cell, it is necessary to specify the sheet material, cell configuration, cell size and effective density. Usually the producers of honeycombs as Hexcel, Plascore, Euro-Composite etc. establish the cell configuration, cell size, material, wall thickness (foil gauge), and nominal density. The density is expresses in pounds per cubic foot (pcf), or kilograms per cubic meter (kg/m^3). The density of the construction solid material is ρ_s, which for aluminum may be considered as 2700 kg/m^3 or 168.55 pcf. As an example, Fig. 2 presents three types of regular aluminum honeycombs produced by Hexcel [16]. The three densities were chosen as: minimum 1 pcf, medium 8.1 pcf, and maximum 22.1 pcf. Therefore, the relative density is calculated in each case. Neglecting the adhesive, the relative density is equal to the ratio between the wall areas of a repetitive cell divided by the area of rectangular material unit cell $L_x \times L_y$. The graphical representation of the cells is presented for comparison.

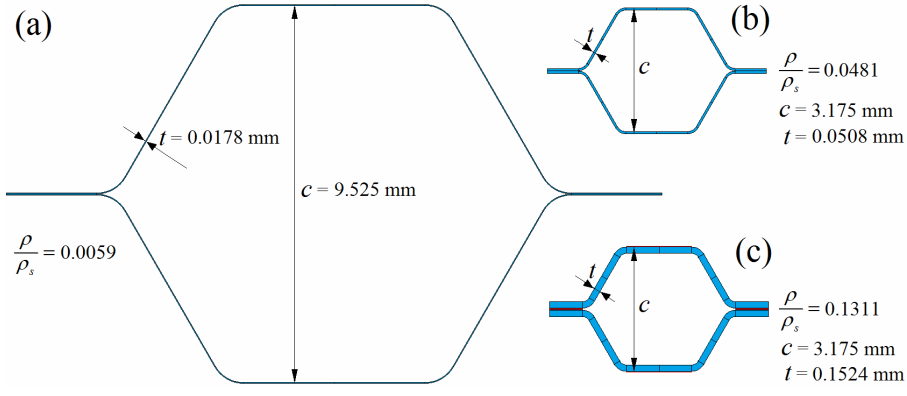

Fig. 2 – Three aluminum commercial honeycombs produced by Hexcel: (a) minimum relative density; (b) medium relative density; (c) maximum relative density. The plots are geometrically scaled one to the other.

3.2 Main cell geometry characterization

The precise characterization of a honeycomb core can be done only experimentally as the final form of the cores depend on the technology of fabrication, expansion or corrugation [1], and the used material.

The number of geometric parameters which completely define by averaging a cell is relatively high. For example, in [12], ten geometric parameters (some depend on the others) were optically identified. However, by considering the previous approaches which consider the cell as symmetric, they can be divided into two categories (Fig. 3): principal parameters,

which define the geometry of the cell – t, ℓ, h, b, θ and R and secondary parameters, which describe the dimensions of the adhesive – t_a, ℓ_a and R_a. Parameter b defines the thickness (height) of the core. These nine geometrically independent parameters define completely a symmetric honeycomb cell with constant wall thickness. They are used through this paper.

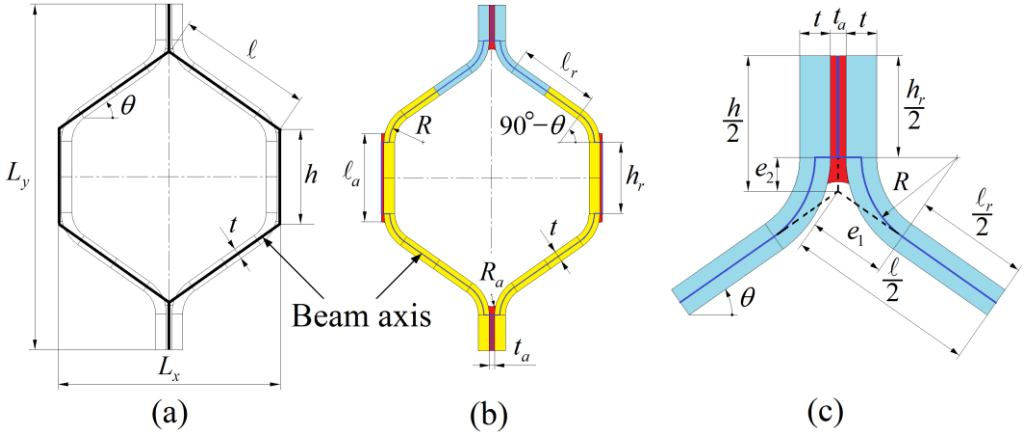

Fig. 3 – Geometric parameters of a commercial honeycomb: (a) classical beam axis model and its parameterization; (b) extended model and parameterization used in this paper; (c) additional dependent geometrical parameters e_1 and e_2

Cell size ($c = L_x$) is measured between two parallel sides of the hexagonal cell [1]. Honeycombs are available in cell sizes ranging from 0.0625 to 1.375 inches (1.6–35 mm). Most common sizes are 0.125, 0.1875, 0.25, 0.375, 0.5, 0.75 and 1.00 in. (around 3, 5, 6, 9, 13, 19 and 25 mm). For hexagonal honeycombs effective densities range from 1 to 22.1 lb/ft^3 (16 to 354 kg/m^3).

Cell wall thicknesses for aluminum, steel and specialty metal honeycombs (titanium, nickel-base alloy, cobalt-base alloy) range from 0.0009 to 0.006 in. (0.02–0.15 mm). Metallic honeycomb cell walls can be either perforated or non-perforated. Various corrosion-resistant coatings are available for aluminum and steel honeycomb. In addition to the substrate, some of the non-metallic honeycombs (kraft paper, aramid, fiberglass and carbon) are reinforced with resin that may be phenolic, polyimide and epoxy. The resin layers increase the density and mechanical properties of the honeycombs. The effective thickness of the wall t can be obtained by averaging the experimental measurements. It is usually given by the producer as a nominal value, which is usually smaller than the effective one [1]. The effective value may be with 15–30% greater than the nominal one.

As to establish the dimensions of a commercial honeycomb, first L_x and L_y are measured directly and averaged. These lengths are measured over lengths of 10 cells and averages are calculated for minimum 6 random locations [1]. For a regular hexagonal core, it should result theoretically that $L_y = \sqrt{3}L_x$ and $\ell^* = \ell = h = L_x/\sqrt{3}$, as well as θ = 30º (Fig. 4a). However, due to technological imperfections these relations are not perfectly satisfied. If the cell size L_x and cell pitch L_y are known, then ℓ, h and θ can be obtained if any of these three parameters or a relation in between them is known. Some practical cases follow.

From Fig. 3a it results:

$$L_x = 2\ell\cos\theta; \qquad L_y = 2\left(h + \ell\sin\theta\right). \tag{2}$$

a) If the internal cell angle θ is known, then from (2) it results:

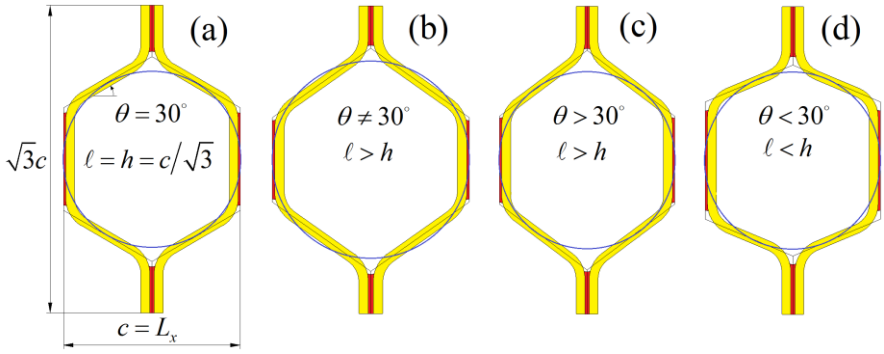

Fig. 4 – Some particular geometries of honeycombs: (a) theoretical model – regular; (b) real – general; please observe that the circle of diameter *c* is not tangent to all middle walls; (c) and (d) particular models – non-regular but tangent to all middle walls

$$\ell = \frac{L_x}{2\cos\theta}, \qquad h = \frac{1}{2}\left(L_y - L_x \tan\theta\right); \tag{3}$$

b) If one establishes $k = h/\ell$, then for $L_y^2 \geq \left(k^2 - 1\right)L_x^2$ it results:

$$\ell = \frac{L_x^2 + L_y^2}{2kL_y + 2\sqrt{\left(1-k^2\right)L_x^2 + L_y^2}}, \quad \theta = arc\cos\left(\frac{L_x}{2\ell}\right). \tag{4}$$

Usually $\ell > h$ (see Fig. 4b), and θ is no more equal to 30º.

c) If the axis of the inclined wall is tangent to the circle of diameter $c = L_x$ (Fig. 4 c,d) then it is possible to obtain two acceptable solutions only if $L_y \geq \sqrt{3}L_x$, which result by applying successively the relations:

$$\theta = 2arc\tan\left(\frac{L_x \pm \sqrt{L_y^2 - 3L_x^2}}{2L_x + L_y}\right), \quad \ell = \frac{L_x}{2\cos\theta}, \qquad h = 2\ell\left(1 - \sin\theta\right). \tag{5}$$

Bitzer mentions that usually $\ell > h$. Instead of $k = h/\ell$ in some papers (see for example [19]) it is used a bondline deviation parameter λ, by which are defined $h = \lambda\ell^*$ and $\ell = \left(2 - \lambda\right)\ell^*$. From the statistical evaluation of the experimental measurements done for Hexcel Al-5052-H39, with cell size 0.375 in (9.525 mm), in [19] the inequality $0.8 \leq \lambda \leq 1.05$ was obtained, giving an average value λ_m = 0.925. The value λ = 1 represents the ideal bond line length. With the notations used in the present paper it results $k = \lambda/\left(2 - \lambda\right)$ and, respectively $0.6667 \leq k \leq 1.1053$, the average value k_m = 0.87 being obtained.

Concerning the radius of curvature *R*, this depends essentially on the process of fabrication and in fact it is not given in the product data sheets of the companies. Masters and Evans [8] established that $R = 0.1\ell$; Balawi and Abot [20], for aluminum honeycombs, suggested that $R = \left(0.2 - 0.4\right)\ell$; Keshavanarayana et al. [12], for a fiberglass/phenolic honeycomb core that was made using a corrugation manufacturing process, showed that precise experimental measurements gave an average $R = 0.2\ell$. For a Nomex honeycomb,

obtained by expansion and impregnated in a phenolic resin, Seeman and Krause [14] used for curvature quantification an indirect parameter named fillet ratio, defined as $y=\left(\ell-\ell_r\right)/2\ell$ for a regular honeycomb only.

Using relations (6), (7) and neglecting the thickness of the walls, it results $R=0.364\ell$ for the value y = 0.21 reported in [14].

In the paper of Kress and Winkler [21] the inclined walls for non-metallic honeycombs obtained through expansion are examined, and it was shown that they are not straight, that is they have a shape of an elongated "*S*" which can be obtained from a beam model having properly chosen boundary conditions.

Although the real shape of the inclined walls is complex, it is reasonable to approximate it as a rectilinear portion in the middle part and two relatively large radii near the nodes ($R\approx\ell$).

This approximation is implying a considerable reduction of the linear part of the wall and of the angle θ obtained for the hypothesis of straight walls.

On the other hand, in the paper of Jang and Kyriakides [22] the shape of an aluminum honeycomb cell was obtained by simulating the process of expansion and the shape of the inclined wall obtained numerically is close to the real one in which the rounded ending part has a relatively small value that is $R<0.1\ell$.

For honeycomb obtained by expansion and then dipped in resins, both the angle θ and the thickness t are not constant, have a great variability and final values are obtained by averaging. In [23], for a Nomex honeycomb material, the cell angle θ was measured in between 26º and 34º.

For the model used in this paper and presented in Figs. 3b, c, the additional geometric parameters e_1 and e_2 are defined and they can be determined without difficulty:

$$e_1=\frac{R\left(1-\sin\theta\right)+\dfrac{t+t_a}{2}}{\cos\theta};\qquad e_2=\frac{R\left(1-\sin\theta\right)-\dfrac{t+t_a}{2}\sin\theta}{\cos\theta}. \tag{6}$$

Then the straight lengths of the cell walls result

$$\ell_r=\ell-2e_1;\qquad h_r=h-2e_2. \tag{7}$$

By considering Fig. 3b, the radius R must be in between the minimum and maximum values geometrically possible. Therefore, the following conditions must be fulfilled simultaneously:

$$R_{\min}\geq\frac{t}{2};\qquad \frac{\ell}{2}-e_1\geq 0 \text{ and } \frac{h}{2}-e_2\geq 0, \tag{8}$$

and the possible domain for which the radius of curvature belongs is

$$\frac{t}{2}\leq R\leq\min\left\{\frac{\ell\cos\theta-\left(t+t_a\right)}{2\left(1-\sin\theta\right)},\frac{h\cos\theta+\left(t+t_a\right)\sin\theta}{2\left(1-\sin\theta\right)}\right\}. \tag{9}$$

3.3 In plane adhesive shape description

The node adhesive is much thicker in the corrugation process than in the expansion process. In fact, the node adhesive in corrugated cores can be 10% of the total honeycomb weight, while it is only about 1% or less in the expanded core [1].

The radius of the adhesive fillet has minimum values if the fillet is tangential to the surfaces of the walls (Fig. 5). Therefore, for $\theta > 0$, if

$$h_r < \ell_a < h_r + (2R+t)\left(1+\cos\theta - \frac{1}{\sin\theta}\right) - \frac{t_a}{\sin\theta}, \tag{10}$$

the junction of the adhesive takes place on the curved part of the inclined walls and the minimum fillet of the adhesive results from the condition

$$R_{a,\min} = \frac{\left(\frac{t_a}{2}\right)^2 + 2\left(R+\frac{t}{2}\right)\frac{t_a}{2} + \left(\frac{\ell_a - \ell_r}{2}\right)^2}{2R + t - \ell_a + \ell_r}. \tag{11}$$

Again, for $\theta > 0$, and if

$$h_r + (2R+t)\left(1+\cos\theta - \frac{1}{\sin\theta}\right) - \frac{t_a}{\sin\theta} < \ell_a < \frac{L_y}{2} + t\cos\theta - \left(\frac{L_x}{2\sin\theta} - t\right)(1-\cos\theta), \tag{12}$$

i.e. junction is to be done on the straight part of the inclined walls, the minimum fillet radius of the adhesive results from the new condition

$$R_{a,\min} = \frac{\frac{\ell_a - h}{2} - \frac{t}{2\cos\theta}}{\tan\theta\tan\frac{\theta}{2}}. \tag{13}$$

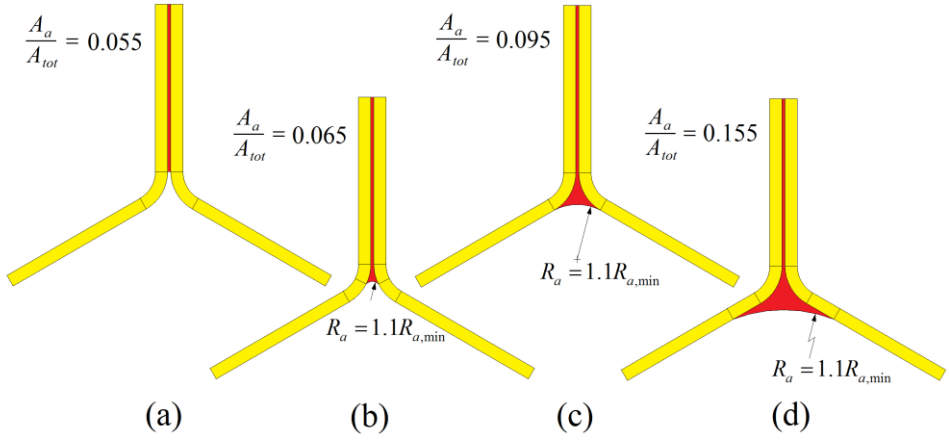

Fig. 5 – Adhesive fillet radius and ratios of adhesive area from total area of a regular honeycomb $\ell/t = 30$; $R = 0.1\ell$ (a) adhesive without fillet ($\ell_a = h_r$); (b) partial adhesive fillet; (c) adhesive full fillet; (d) in excess adhesive fillet

The two relations to be used to estimate the minimum radius of curvature of the adhesive fillet (11) and (13) depend on the effective length of the adhesive. In fact, the adhesive fillet radius established experimentally can start from the curved or from the straight part of the wall.

In this paper, the radius of the adhesive fillet is considered $R_a = 1.1R_{a,\min}$, both from the condition of adherence, as the adhesive intersects the wall at an angle different from zero,

and to reduce the distortion of the finite elements which model the adhesive at the junction between the adhesive and the walls where a sharp angle appears.

3.4 Honeycomb cell materials

The properties of the cell wall material and node bond adhesive are seldom available in the public domain.

To facilitate the numerical modeling of the cells, it is necessary to know the mechanical properties of the cell wall material and the node bond adhesive [12].

In the componence of the core there are at least two different materials: sheet material and adhesive.

Sheets are from metals or composite materials. For metals the material properties are usually known, although it is possible that for very thin sheets, properties are different than from the ones established on standardized specimens.

Small differences may also result due to the presence of corrosion-resistant coatings. For composite walls the material properties may be different from one producer to another. As an example, Roy et al. [13] obtained experimentally the mechanical properties of a Nomex honeycomb core constituents using tensile tests and the strain gage method. They found that paper coated with phenolic resin properties are dependent on the paper's nominal thickness and that the material is orthotropic. Similar orthotropic properties were reported also by Seemann and Krause [14].

The average values reported in the open literature by Keshavanarayana et al. [12] for node bond adhesive, which is made of phenolic resin, were E_a = 3.79 GPa and ν_a = 0.38. From da Silva and Adams [24] one can conclude that at normal temperature, for structural adhesives E_a = 2–7 GPa.

From other references [25–27] it can be concluded than from flexible to rigid adhesives the range of the elastic properties the adhesives are E_a = 1 MPa–10 GPa and ν_a = 0.3–0.49.

3.5 Honeycomb density calculation

As the thickness (height) of the core b is constant, the effective (homogenized) density ρ results as

$$\rho = \frac{\rho_s A_s + \rho_a A_a}{L_x L_y}, \tag{14}$$

where the total area of the walls sections A_s, and the area of the adhesive A_a, is resulting by the summation of the areas rectangles and sectors of circle (see Fig. 3b), that is:

$$A_s = 4t\left[h_r + \ell_r + (\pi - 2\theta)R\right]; \quad A_a = 2t_a h_r . \tag{15}$$

The lengths of the rectilinear parts h_r and ℓ_r are expressed as a function of the geometric parameters which define the geometry in Eq. (7).

4. ANALYTICAL EQUATIONS

For a honeycomb structure (Fig. 1) of large dimensions, theoretically infinite, where adhesive and curvature radius at the inclined cell walls are neglected, loaded as LC 1, LC 2 and LC 3 in Table 1, analytical relationships for homogenization of commercial hexagonal honeycombs are [2]:

$$\frac{\rho}{\rho_s}=\frac{\frac{t}{\ell}\left(\frac{h}{\ell}+1\right)}{\left(\frac{h}{\ell}+\sin\theta\right)\cos\theta};\ E_3=E_s\frac{\rho}{\rho_s};\qquad \nu_{31}=\nu_{32}=\nu_s, \tag{16}$$

$$G_{13}=G_s\left(\frac{t}{\ell}\right)\frac{\cos\theta}{\left(\frac{h}{\ell}+\sin\theta\right)};\qquad G_{23}=G_{23}^{LB}+\frac{\alpha}{\left(\frac{b}{\ell}\right)}\left(G_{23}^{UB}-G_{23}^{LB}\right) \tag{17}$$

where

$$\alpha=\begin{cases}0.787 & \theta\geq 0^\circ\\ 1.342 & \theta<0^\circ\end{cases};\quad G_{23}^{UB}=G_s\left(\frac{t}{\ell}\right)\frac{\frac{h}{\ell}+\sin^2\theta}{\left(\frac{h}{\ell}+\sin\theta\right)\cos\theta};\ G_{23}^{LB}=G_s\left(\frac{t}{\ell}\right)\frac{\frac{h}{\ell}+\sin\theta}{\left(\frac{h}{\ell}+1\right)\cos\theta}. \tag{18}$$

For regular honeycombs ($\ell=h$ and θ =30º) from (17) and (18) it yields

$$\frac{G_{23}}{G_{13}}=1.5\left[1+0.08744\left(\frac{\ell}{b}\right)\right], \tag{19}$$

and for $b>\ell$ we obtain $G_{23}/G_{13}\approx 1.5$.

Nevertheless, if we look at the experimental results reported by producers [16, 17], this ratio is 1.7 – 4.4, with a mean around 2.

One reason of this discrepancy may be due to simplified hypotheses used in obtaining (17) and (18) i.e. neglecting the adhesive layer and the curvature radius *R*.

Analytical relationships for G_{23} and G_{13} considering the real geometry of honeycombs are difficult to be obtained, and numerical methods may be used as an alternative.

5. FINITE ELEMENT ANALYSIS FOR HOMOGENIZATION

For determining the effective elastic constants by using FEA we developed the finite element models for a representative volume element (RVE), i.e. 1/8 of the repetitive unit cell (see Fig. 6) due to the geometric symmetry, symmetry or anti-symmetry of loads, respectively.

Then, according to Sorohan et al. [6], for an out-of-plane study may be defined only three loading cases (LCs) from which it can be establish all the five out-of-plane effective constants of the material using the boundary conditions presented in Table 2.

The considered LCs correspond to those which define the elastic constants of an orthotropic material (Table 1). From the finite element model the relative density of the core can be effortlessly obtained. Comparing to what was reported in [6], this model differs only as geometry, radius of curvature and the adhesive were included in the finite element mesh. For a more precise numerical model only Brick elements are considered. The arbitrarily imposed averaged strains were considered equal for all load cases: $\bar{\varepsilon}_3=\bar{\gamma}_{23}=\bar{\gamma}_{13}=0.01$.

For FEA calculations the software ANSYS 19.0 in classic version was used, and APDL command files were generated as to parametrically describe various honeycomb configurations. More explanations on the modeling and obtained results were presented in [6, 7, 15].

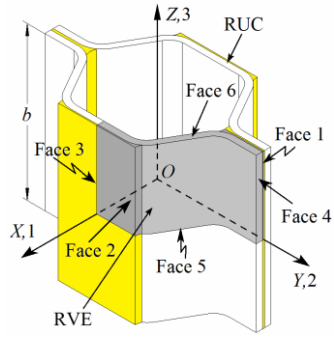

Fig. 6 – Global system of coordinates O*XYZ* which coincide with principal directions of equivalent orthotropic material 123, and notation of faces implied by the BC for the repetitive unit cell and for RVE which are considered in finite element analysis

Table 2 – Displacement boundary conditions for the three load cases for Free | Rigid skin effect used in simulations

Load Case	Nodes on Face	u_x	u_y	u_z	Remark
1 Axial Z	1 ($X=0$)	0	Free	Free	Sym X
	2 ($X=L_x/2$)	Coupled | 0	Free	Free	-
	3 ($Y=0$)	Free	0	Free	Sym Y
	4 ($Y=L_y/2$)	Free	Coupled | 0	Free	-
	5 ($Z=0$)	Free	Free	0	Sym Z
	6 ($Z=b/2$)	Free | 0	Free | 0	$\bar{\varepsilon}_3 b/2$	-
2 Shear YZ	1 ($X=0$)	0	Free	Free	Sym X
	2 ($X=L_x/2$)	0	Free	Free	-
	3 ($Y=0$)	0	Free	0	ASym Y
	4 ($Y=L_y/2$)	0	Free	0	-
	5 ($Z=0$)	0	0	Free	ASym Z
	6 ($Z=b/2$)	Free | 0	$\bar{\gamma}_{23} b/2$	Free | 0	-
3 Shear XZ	1 ($X=0$)	Free	0	0	ASym X
	2 ($X=L_x/2$)	Free	0	0	-
	3 ($Y=0$)	Free	0	Free	Sym Y
	4 ($Y=L_y/2$)	Free	0	Free	-
	5 ($Z=0$)	0	0	Free	ASym Z
	6 ($Z=b/2$)	$\bar{\gamma}_{13} b/2$	Free | 0	Free | 0	-

6. RESULTS AND DISCUSSIONS

6.1 Case study

Three honeycombs with different relative densities, as presented in Fig. 2, correspond to hexagonal honeycombs produced by Hexcel [16] of what we considered as being: minimum density, medium density, and maximum density. The geometries of the cells and the materials' properties are given in Table 3 and Table 4, respectively. The cells are not completely defined in [16], so they are slightly corrected according to available information as to obtain the nominal densities given by the producer. As the adhesive was not explicitly established, a ratio of the elastic moduli was adopted as E_s/E_a = 20.

Table 3 – Geometric parameters for three commercial honeycombs considered in case study (see Fig. 2 and Fig. 3)

Hexagonal Honeycomb	$c=L_x$ [mm]	t [mm]	θ [°]	$\ell = h$ [mm]	R [mm]	t_a [mm]	$\ell_a = h_r$ [mm]	b [mm]	R_a [mm]
Hexcel 1.0–3/8–.0007 Minimum density	9.525	0.021	30	5.500	1.375	0.008	3.929	15.875	∞
Hexcel 8.1–1/8–.002 Medium density	3.175	0.058	30	1.833	0.500	0.016	1.298	15.875	∞
Hexcel 22.1–1/8–.006 Maximum density	3.175	0.160	30	1.833	0.500	0.061	1.383	15.875	∞

Table 4 – Material constants for the aluminum and adhesive for honeycombs given in Table 3

Material	Young's modulus [MPa]	Poisson ratio [-]	Mass density [kg/m^3]
Aluminum	E_s = 70000	ν_s = 0.33	ρ_s = 2700
Adhesive	E_a = 3500	ν_a = 0.38	ρ_a = 1500

For the three sets of analyzed data, all available experimental data and some results are presented in Tables 5–7, each for one density. Node adhesive percent weight w_a of the total honeycomb, is also presented in the tables. The analytical results for out-of-plane effective constant are not available, instead two analytical approaches which completely neglect the adhesive layer and the curvature radius of the inclined wall at intersection were used for a first estimation [2, 6]. "FREE" corresponds to the neglect of the skin effect and "SKIN" to the rigid skin effect. The numerical results obtained with FEA used Brick8 elements and the excess of adhesive was neglected (see Fig. 5a and Table 3). From a convergence analysis it was found that 2 layers of elements over the thickness of the wall t and 2 layers over the adhesive thickness t_a are enough to obtain a good convergence. If the type of element is changed to Brick20, practically the same results are obtained for this last refined mesh. The reference results in this paper are considered the experimental ones, although these may be affected by some errors [28, 29].

Table 5 – Results obtained for minimum density (relative density 0.0059)

Effective constant	Experimental HEXCEL (1999)	Analytic - Adhesive layer and curvature radius R neglected		Numerical - FEA	
		FREE - Generalized Malek and Gibson (2018)	SKIN - Gibson and Ashby (1997)	FREE	SKIN
ρ [kg/m^3]	16	15.8	15.9	16.0	16.0
w_a [%]	-	0	0	3.74	3.74
E_3 [MPa]	69-103*	411	411	401	401
G_{23} [MPa]	83-103*	81	90	23	92
G_{13} [MPa]	47-48*	51	58	24	47
ν_{32} [-]	-	0.33	0.33	0.33	0.33
ν_{31} [-]	-	0.33	0.33	0.33	0.33

* This range of variation corresponds to different materials: aluminum 5052 and respectively 5056

Table 6 – Results obtained for medium density (relative density 0.048)

Effective constant	Experimental HEXCEL (1999)	Analytic - Adhesive layer and curvature radius R neglected		Numerical - FEA	
		FREE - Generalized Malek and Gibson (2018)	SKIN - Gibson and Ashby (1997)	FREE	SKIN
ρ [kg/m^3]	130	130	132	130	130
w_a [%]	-	0	0	2.75	2.75
E_3 [MPa]	2413	3379	3410	3277	3277

G_{23} [MPa]	931	718	728	644	759
G_{13} [MPa]	372	477	481	327	369
v_{32} [-]	-	0.33	0.33	0.33	0.33
v_{31} [-]	-	0.33	0.33	0.33	0.33

Table 7 – Results obtained for maximum density (relative density 0.131)

Effective constant	Experimental HEXCEL (1999)	Analytic - Adhesive layer and curvature radius *R* neglected		Numerical - FEA	
		FREE - Generalized Malek and Gibson (2018)	SKIN - Gibson and Ashby (1997)	FREE	SKIN
ρ [kg/m^3]	354	354	363	354	354
w_a [%]	-	0	0	4.09	4.09
E_3 [MPa]	6688	9170	9407	8830	8830
G_{23} [MPa]	3034	2017	2009	1936	2154
G_{13} [MPa]	690	1363	1326	826	918
v_{32} [-]	-	0.33	0.33	0.33	0.33
v_{31} [-]	-	0.33	0.33	0.33	0.33

If the minimum density is analyzed, it is to be noticed that the maximum errors obtained correspond to the Young modulus E_3, which results over 4 times larger than experimental result. The remaining results are very close to the numerical ones for the rigid skin effect. For the medium and maximum densities, the numerical results are relatively close to the experimental data except E_3 and G_{23}. Analytical results are reasonably considering the simplified geometries and neglecting the adhesive layer, but, for example in Table 7, it can be seen that G_{13} is almost two times larger. Some additional errors come from the "guess" of the inputs considered in Table 3 and Table 4.

6.2 Sensitivity analysis

Because the ratio G_{23}/G_{13} of the experimental results may be much over 1.5 as in the analytical approach (see chapter 4) and over 2 as it was obtained in the numerical approach (see Table 7, where 3034/690=4.4), a sensitivity analysis using FEA was performed, considering in turn as variable R, t_a, ℓ_a and E_a, parameters which were neglected in the analytical theory. Some parameters as R_a and v_a are not practically sensitive to the elastic out-of-plane moduli. Only the case of maximum relative density is considered for this study.

6.2.1 Cell curvature radius variation

The honeycomb model is defined in this paragraph by the geometric parameters from Table 3 – last row, and material parameters from Table 4, except the adhesive length which was considered more realistic, i.e. ℓ_a = 1.75 mm.

It must be mentioned that due to larger adhesive length the out-of-plane moduli result a little bit larger than the values presented in Table 7; at the same time some parameters as w_a, R_a and ρ will change, but their variations are relatively small comparing to the initial values obtained for inputs in Tables 3 and 4.

Also the variations of the out-of-plane Poisson's ratios v_{32} and v_{31} are insignificant. The variations of the out-of-plane moduli are presented in Fig. 7a. The most sensitive is G_{13}, which for rigid skin effect, reduces from 1031 MPa to 931 MPa when R increases from 0.1 mm to 1.35 mm.

In the same range of variation for R, G_{23} increases from 2121 MPa to 2278 MPa and E_3 decreases from 9061 MPa to 8444 MPa.

6.2.2 Adhesive thickness variation

For the same parameters as in previous paragraph, only the adhesive thickness t_a was considered variable in the range 0.1t–1.1t.

The variations of the out-of-plane moduli are presented in Fig. 7b. Also, the most sensitive is G_{13}, which for rigid skin effect, reduces from 1114 MPa to 888 MPa when t_a increases from 0.016 mm to 0.176 mm.

In the same range of variation, G_{23} increases from 2136 MPa to 2217 MPa and E_3 decreases from 8883 MPa to 8759 MPa.

6.2.3 Adhesive length variation

With all inputs as in Table 3 and Table 4, considering ℓ_a variable in the range 0.25 mm–2.25 mm, the obtained sensitivity curves are plotted in Fig. 7c. Again, the most sensitive is G_{13}, which for rigid skin effect, increases from 549 MPa to 1121 MPa when ℓ_a increases in the imposed limits. In the same range of ℓ_a variation, G_{23} increases only from 2143 MPa to 2167 MPa and E_3 increases from 8806 MPa to 8903 MPa.

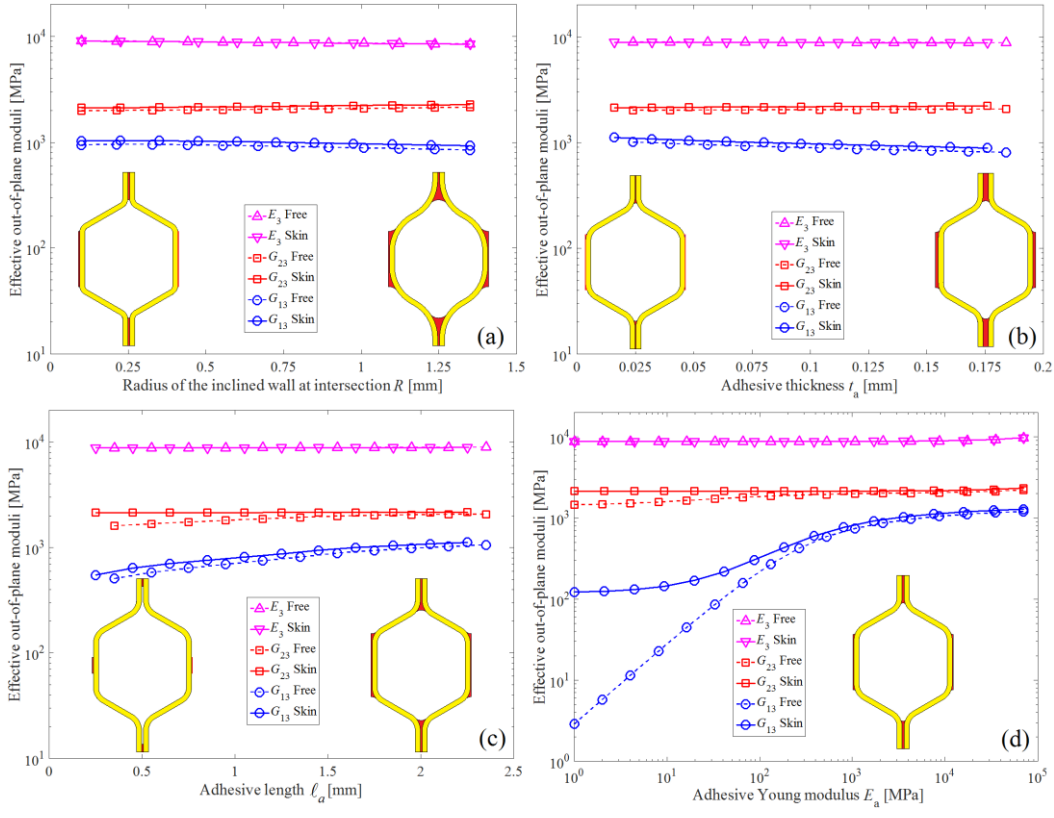

Fig. 7 – Sensitivity analysis of out-of-plane moduli. (a) function of R; (b) function of t_a; (c) function of ℓ_a; (d) function of E_a

6.2.4 Adhesive Young's modulus variation

Considering the same constant parameters as in §6.2.1 and only E_a variable in the hypothetical range 1 MPa – 70 GPa, the obtained sensitivity curves are plotted in Fig. 7d. It is clear that G_{13} is very sensitive to the adhesive elasticity especially in the range of elastic

adhesives E_a = 10 – 500 MPa. G_{13}, for rigid skin effect, increases from around of 450 MPa to 1020 MPa, when E_a increases from 200 MPa to 3500 MPa. In the same range of variation for E_a, G_{23} increases only from 2145 MPa to 2157 MPa and E_3 increases only from 8806 MPa to 8847 MPa.

7. SUMMARY AND CONCLUSIONS

A general parameterization of a periodic hexagonal honeycomb with double vertical walls considering their radius of curvature and adhesive layer at nodes was proposed. All five effective out-of-plane elastic properties were obtained using FEA and some of them were validated by experimental results.

It is necessary to realize a detailed analysis of the structure of the honeycomb which must be homogenized. It is of a crucial importance to establish: the technology of fabrication of the honeycomb, the materials properties of the walls and of the adhesive, as well as the correct measurement/averaging of the walls thickness, cell dimensions, radius of curvature of the inclined walls, but also of the quantity and fillet of the adhesive. A first verification, very important, must allow obtaining through calculations the relative density and adhesive mass percentage from the honeycomb total mass. The sensitivity analyses show that the most sensitive parameter which modifies the ratio G_{23}/G_{13} is the adhesive Young modulus E_a, but also the adhesive length ℓ_a and its thickness t_a may be important.

ACKNOWLEDGEMENTS

The authors acknowledge the support given by a grant of the Romanian National Authority for Scientific Research and Innovation CCCDI-UEFISCDI, project number 11/2015.

REFERENCES

[1] T. Bitzer, *Honeycomb Technology: Materials, Design, Manufacturing, Applications and Testing*, Chapman & Hall, London,1997.

[2] L. J. Gibson and M. F. Ashby, *Cellular Solids, Structure and Properties*, second ed. Cambridge University Press, New York, 1997.

[3] W. S. Burton and A. K. Noor, Assessment of continuum models for sandwich panel honeycomb cores, *Computational Methods in Applied Mechanics and Engineering*, vol. **145**, pp. 341–360, 1997.

[4] S. Balawi and J. L. Abot, The effect of honeycomb relative density on its effective in-plane elastic moduli: An experimental study, *Composite Structures*, vol. **84**, 293–299, 2008.

[5] A. Karakoç and J. Freund, Experimental studies on mechanical properties of cellular structures using Nomex honeycomb cores, *Composite Structures*, vol. **94**, 2017–2024, 2012.

[6] St. Sorohan, D. M. Constantinescu, M. Sandu and A. G. Sandu, On the homogenization of hexagonal honeycombs under axial and shear loading. Part I: analytical formulation for free skin effect, *Mechanics of Materials*, vol. **119**, 74–91, 2018.

[7] St. Sorohan, D. M. Constantinescu, M. Sandu and A. G. Sandu, On the homogenization of hexagonal honeycombs under axial and shear loading. Part II: comparison of free skin and rigid skin effects on effective core properties, *Mechanics of Materials*, vol. **119**, pp. 92–108, 2018.

[8] I. G. Masters and K. E. Evans, Models for the elastic deformation of honeycombs, *Composite Structures*, vol. **35**, pp. 403-422, 1996.

[9] A. Catapano and M. Montemurro, A multi-scale approach for the optimum design of sandwich plates with honeycomb core. Part I: homogenisation of core properties, *Composite Structures*, vol. **118**, pp. 664–676, 2014.

[10] S. Malek and L. Gibson, Effective elastic properties of periodic hexagonal honeycombs, *Mechanics of Materials*, vol. **91**, pp. 226–240, 2015.

[11] K. Qiu, Z. Wang and W. Zhang, The effective elastic properties of flexible hexagonal honeycomb cores with consideration for geometric nonlinearity, *Aerospace Science and Technology*, vol. **58**, pp. 258–266, 2016.
[12] S. R. Keshavanarayana, H. Shahverdi, A. Kothare, C. Yang and J. Bingenheimer, The effect of node bond adhesive fillet on uniaxial in-plane responses of hexagonal honeycomb core, *Composite Structures*, vol. **175**, pp. 111–122, 2017.
[13] R. Roy, S.-J. Park, J.-H. Kweon and J.-H. Choi, Characterization of Nomex honeycomb core constituent material mechanical properties, *Composite Structures*, vol. **117**, pp. 255–266, 2014.
[14] R. Seemann and D. Krause, Numerical modelling of Nomex honeycomb sandwich cores at meso-scale level, *Composite Structures*, vol. **159**, pp. 702–718, 2017.
[15] St. Sorohan, D. M. Constantinescu, M. Sandu and A.G. Sandu, In-plane homogenization of commercial hexagonal honeycombs considering the cell wall curvature and adhesive layer influence, *International Journal of Solids and Structures*, https://doi.org/10.1016/j.ijsolstr.2018.08.007, 2018.
[16] * * * HexWeb™, *Honeycomb attributes and properties - A comprehensive guide to standard Hexcel honeycomb materials, configurations, and mechanical properties*, Hexcel Corporation, 1999.
[17] * * * Plascore®, 2017. PAMG-XR1 5052 Aluminum Honeycomb. https://www.plascore.com /download/datasheets/honeycomb_data_sheets/Plascore_PAHD-XR1_5052.pdf (last accessed 7 February 2018).
[18] J. Kindinger, *Lightweight Structural Cores*, in ASM Handbook Vol. **21**: Composites, ASM International, 2001.
[19] A. Wilbert, W.-Y. Jang, S. Kyriakides and J.F. Floccari, Buckling and progressive crushing of laterally loaded honeycomb, *International Journal of Solids and Structures*, vol. **48**, pp. 803–816, 2011.
[20] S. Balawi and J.L. Abot, A refined model for the effective in-plane elastic moduli of hexagonal honeycombs. *Composite Structures*, vol. **84**, pp. 147–158, 2008.
[21] G. Kress and M. Winkler, Honeycomb sandwich residual stress deformation pattern, *Composite Structures*, vol. **89**, pp. 294–302, 2009.
[22] W. Y. Jang and S. Kyriakides, On the buckling and crushing of expanded honeycomb, *International Journal of Mechanical Sciences*, vol. **91**, pp. 81–90, 2015.
[23] A. Karakoç, K. Santaoja and J. Freund, Simulation experiments on the effective in-plane compliance of the honeycomb materials, *Composite Structures*, vol. **96**, pp. 312–320, 2013.
[24] L. F. M. da Silva and R. D. Adams, Measurement of the mechanical properties of structural adhesives in tension and shear over a wide range of temperatures, *Journal of Adhesion Science and Technology*, vol. **19**, pp. 109–141, 2005.
[25] D. A. Dillard and A. X. Pocius (Eds.), *The Mechanics of Adhesion*, Elsevier, Amsterdam, 2002.
[26] B. Hussey and J. Wilson, *Structural Adhesives*, Chapman & Hall, 1996.
[27] A. Pizzi and K. L. Mittal (Eds.), *Handbook of Adhesive Technology*, second ed. revised and expanded, Marcel Dekker, New York·Basel, 2003.
[28] * * * ASTM C273 2000, *Standard method of shear test in flatwise plane of flat sandwich constructions or sandwich cores*, West Conshohocken, Pa., USA.
[29] * * * ASTM C365 1988, *Standard test methods for flatwise compressive strength of sandwich cores*, West Conshohocken, Pa., USA.